ELSEVIER

European Journal of Pharmacology 380 (1999) 153–162

ejp

www.elsevier.nl/locate/ejphar

Resolution, absolute stereochemistry and molecular pharmacology of the enantiomers of ATPA

Tine B. Stensbøl [a], Lars Borre [c], Tommy N. Johansen [a], Jan Egebjerg [c], Ulf Madsen [a], Bjarke Ebert [b], Povl Krogsgaard-Larsen [a,*]

[a] *PharmaBiotec NeuroScience Research Center, Department of Medicinal Chemistry, The Royal Danish School of Pharmacy, 2 Universitetsparken, DK-2100 Copenhagen, Denmark*

[b] *PharmaBiotec NeuroScience Research Center, Department of Pharmacology, The Royal Danish School of Pharmacy, 2 Universitetsparken, DK-2100 Copenhagen, Denmark*

[c] *Department for Molecular and Structural Biology, University of Aarhus, Aarhus, Denmark*

Received 15 April 1999; received in revised form 28 June 1999; accepted 13 July 1999

Abstract

(*RS*)-2-Amino-3-(5-*tert*-butyl-3-hydroxy-4-isoxazolyl)propionic acid (ATPA), an analogue of (*RS*)-2-amino-3-(3-hydroxy-5-methyl-4-isoxazolyl)propionic acid (AMPA), has previously been shown to be a relatively weak AMPA receptor agonist and a very potent agonist at the GluR5 subtype of kainic acid-preferring (*S*)-glutamic acid ((*S*)-Glu) receptors. We report here the separation of (+)- and (−)-ATPA, obtained at high enantiomeric purity (enantiomeric excess values of 99.8% and >99.8%, respectively) using chiral chromatography, and the unequivocal assignment of the stereochemistry of (*S*)-(+)-ATPA and (*R*)-(−)-ATPA. (*S*)- and (*R*)-ATPA were characterized in receptor binding studies using rat brain membranes, and electrophysiologically using the rat cortical wedge preparation and cloned AMPA-preferring (GluR1, GluR3, and GluR4) and kainic acid-preferring (GluR5, GluR6, and GluR6 + KA2) receptors expressed in *Xenopus* oocytes. In the cortical wedge, (*S*)-ATPA showed AMPA receptor agonist effects (EC_{50} = 23 μM) approximately twice as potent as those of ATPA. (*R*)-ATPA antagonized depolarizations induced by AMPA (K_i = 253 μM) and by (*S*)-ATPA (K_i = 376 μM), and (*R*)-ATPA antagonized the biphasic depolarizing effects induced by kainic acid (K_i = 301 μM and 1115 μM). At cloned AMPA receptors, (*S*)-ATPA showed agonist effects at GluR3 and GluR4 with EC_{50} values of approximately 8 μM and at GluR1 (EC_{50} = 22 μM), producing maximal steady state currents only 5.4–33% of those evoked by kainic acid. (*R*)-ATPA antagonized currents evoked by kainic acid at cloned AMPA receptor subtypes with K_i values of 33–75 μM. (*S*)-ATPA produced potent agonist effects at GluR5 (EC_{50} = 0.48 μM). Due to desensitization of GluR5 receptors, which could not be fully prevented by treatment with concanavalin A, (*S*)-ATPA-induced agonist effects were normalized to those of kainic acid. Under these circumstances, maximal currents produced by (*S*)-ATPA and kainic acid were not significantly different. (*R*)-ATPA did not attenuate currents produced by kainic acid at GluR5, and neither (*S*)- nor (*R*)-ATPA showed significant effects at GluR6. (*S*)-ATPA as well as AMPA showed weak agonist effects at heteromeric GluR6 + KA2 receptors, whereas (*R*)-ATPA was inactive. Thus, (*S*)- and (*R*)-ATPA may be useful tools for mechanistic studies of ionotropic non-NMDA (*S*)-Glu receptors, and lead structures for the design of new subtype-selective ligands for such receptors.

Keywords: AMPA (2-amino-3-(3-hydroxy-5-methyl-4-isoxazolyl)propionic acid); ATPA (2-amino-3-(5-*tert*-butyl-3-hydroxy-4-isoxazolyl)propionic acid); Kainic acid; Chiral chromatography; Enantiomer; AMPA receptor cloned; Kainate receptor cloned; Cortical wedge preparation; (Rat)

1. Introduction

(*S*)-Glutamic acid ((*S*)-Glu) is the major excitatory amino acid in the central nervous system. (*S*)-Glu operates through multiple ionotropic and G-protein coupled metabotropic receptors (Collingridge and Watkins, 1994; Wheal and Thomson, 1995; Krogsgaard-Larsen et al., 1996; Conn and Pin, 1997; Monaghan and Wenthold, 1997). It is generally agreed that both ionotropic and metabotropic (*S*)-Glu receptors play important roles in the neuronal transmission in the central nervous system (CNS), and that all subtypes of these receptors are potential targets for therapeutic intervention in a number of CNS diseases (Danysz et al., 1995; Knöpfel et al., 1995). The ionotropic

* Corresponding author. Tel.: +45-35306511; fax: +45-35306040; E-mail: nordly@medchem.dfh.dk

0014-2999/99/$ - see front matter
PII: S0014-2999(99)00512-9

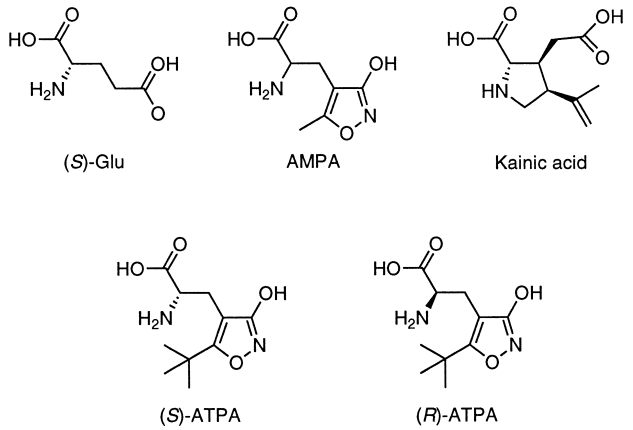

Fig. 1. Structures of (*S*)-glutamic acid ((*S*)-Glu) and some heterocyclic analogues.

receptors are divided into three heterogenous classes of receptors: *N*-methyl-D-aspartic acid (NMDA), (*RS*)-2-amino-3-(3-hydroxy-5-methyl-4-isoxazolyl)propionic acid (AMPA) and kainic acid receptors. Molecular biological studies have identified four AMPA-preferring subunits, GluR1–GluR4, and two groups of kainic acid-preferring subunits, KA1 and KA2 and GluR5–GluR7 (Hollmann and Heinemann, 1994). AMPA and kainic acid receptors are often named non-NMDA receptors due to the lack of specific ligands. Thus, there is a need for highly selective agonists and antagonists for AMPA and kainic acid receptors as pharmacological tools and potential therapeutic agents.

(*RS*)-2-Amino-3-(5-*tert*-butyl-3-hydroxy-4-isoxazolyl)propionic acid (ATPA) (Fig. 1) has previously been described as an AMPA receptor agonist markedly weaker than AMPA (Lauridsen et al., 1985; Ebert et al., 1992). In contrast to AMPA, ATPA is capable of passing the blood brain–barrier (Arnt et al., 1995), most likely due to the more lipophilic character of this agonist. Clarke et al. (1997) have described the racemate of ATPA as a highly potent and selective agonist at the kainic acid-preferring GluR5 subtype of ionotropic (*S*)-Glu receptors. Recently, a preliminary electrophysiological characterization of the optical isomers of ATPA has been reported (Curry and Pajouhesh, 1998). We report here the chiral separation of ATPA, the establishment of the absolute stereochemistry, and a detailed in vitro electrophysiological characterization of (*S*)-ATPA and (*R*)-ATPA (Fig. 1), using the rat cortical wedge preparation as well as cloned AMPA- and kainic acid-preferring receptors.

2. Materials and methods

2.1. Chemicals and analytical and spectroscopic techniques

[^{3}H]AMPA (53.1 Ci/mmol), [^{3}H]-6-cyano-7-nitroquinoxaline-2,3-dione ([^{3}H]CNQX) (24.6 Ci/mmol), [^{3}H]kainic acid (58.0 Ci/mmol), and [^{3}H]-3-(2-carboxypiperazin-4-yl)propyl-1-phosphonic acid ([^{3}H]CPP) (36.0 Ci/mmol) were purchased from New England Nuclear (Boston, MA, USA). All other chemicals were synthesized according to previously described procedures or purchased through standard commercial sources. Elemental analyses were performed by the Analytical Research Department (H. Lundbeck, Copenhagen, Denmark) and are within 0.4% of the calculated values. ^{1}H Nuclear Magnetic Resonance (NMR) spectra were recorded on a Gemini 2000 BB, 300-MHz spectrometer and infrared (IR) spectra were recorded from KBr disks on a Perkin-Elmers 781 grating infrared spectrophotometer. Optical rotations were measured in thermostated cuvettes on a Perkin-Elmer 241 polarimeter and circular dichroism (CD) spectra were recorded in 1.0-cm cuvettes at room temperature on a Jasco J-720 spectropolarimeter.

2.2. Chiral chromatographic techniques

In experiments using the Chirobiotic T columns (4.6 × 150 mm or 10 × 500 mm, ASTEC, Whippany, NJ), the high performance liquid chromatography (HPLC) system consisted of a Waters pump (model 590) connected to a Rheodyne injector (model 7125), equipped with a 20-μl or a 5-ml loop, respectively, a Waters UV-detector (model 481) and a Hitachi D-2000 chromato-integrator. Analytical and preparative HPLC experiments using the Chirobiotic T columns were carried out using 15 mM ammonium acetate/acetic acid buffer (pH 4.0): ethanol (80:20) with a flowrate of 0.5 ml/min and 2.0 ml/min, respectively. In preparative experiments, a guard column (4.6 × 50 mm) was used prior to the 10 × 500-mm column. In experiments using an (*S*)-pipecolic acid ligand-exchange column (4.6 × 120 mm), prepared in accordance with the procedure described by Gübitz et al. (1981a), the HPLC system consisted of a Waters pump (model 510) connected to a Waters U6K injector and a Waters photodiode array detector (model 991). The temperature was kept at 50°C and the eluting buffer was 50 mM KH_2PO_4 containing 0.125 mM $CuSO_4$. The flowrate was 1.0 ml/min. UV-detection was in all HPLC experiments carried out at 225 nm.

2.3. Resolution and configurational assignment of (S)-ATPA and (R)-ATPA

Two hundred milligrams of racemic ATPA was dissolved in 25 mM aqueous ammonia (5 mg/ml), resulting in a solution with pH 8. Upon filtration through Millipore filters 0.45 μM, 2 ml (10 mg) was injected per run, and was separated into two fractions, the first fraction containing the (+)-enantiomer and second fraction containing the (−)-enantiomer (Fig. 2A). The pooled fractions containing each enantiomer were evaporated and re-evaporated three times from water. Upon recrystallization from water, the first eluting enantiomer afforded (+)-ATPA (42 mg, 42%;

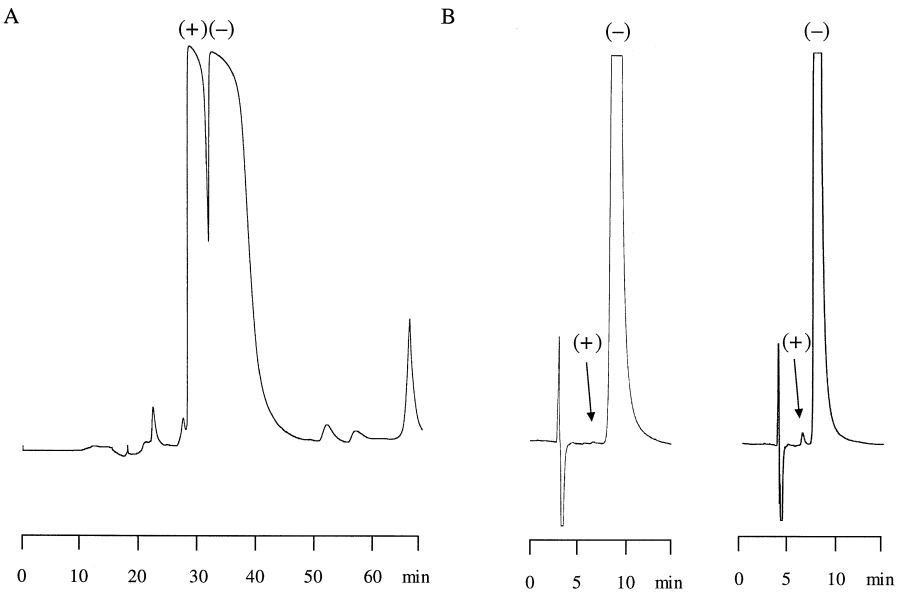

Fig. 2. Chiral HPLC chromatograms. (A) Separation of 10 mg ATPA using a Chirobiotic T column (10 × 500 mm). (B) Injection of (−)-ATPA (left) and injection of (−)-ATPA spiked with a small amount of racemic ATPA (right), both on a Chirobiotic T column (4.6 × 150 mm).

enantiomeric excess (ee) = 99.8%), and after recrystallization of the mother liquor a second crop of crystals of 10 mg (10%; ee = 99.8%). $[\alpha]_D^{24} = +30.6°$ ($c = 0.43$, 1 M HCl). Anal.: $C_{10}H_{16}O_4N_2$: C, H, N. The second eluting enantiomer gave 55.4 mg of (−)-ATPA (55%; ee > 99.8%) after recrystallization from water and a second crop of 6 mg (6%; ee = 99.5%) after recrystallization of the mother liquor. $[\alpha]_D^{24} = -29.8°$ ($c = 0.40$, 1 M HCl). Anal.: $C_{10}H_{16}O_4N_2$: C, H, N. ^{1}H NMR and IR spectra of (+)- and (−)-ATPA were identical and similar to those of racemic ATPA (Lauridsen et al., 1985). The CD-spectra of (+)- and (−)-ATPA clearly illustrated that the two compounds are enantiomers. The CD-spectra of (+)-ATPA ($c = 0.2$ mM, 0.1 M HCl) showed a positive Cotton-effect at 220 nm ($\Delta\varepsilon = +0.13$ m^2/mol), whereas that of the (−)-enantiomer showed a negative Cotton-effect at the same wavelength.

The configurational assignment was accomplished by converting (*R*)-2-amino-3-(5-*tert*-butyl-3-phosphonomethoxy-4-isoxazolyl)propionic acid ((*R*)-ATPO) (Fig. 3) into (*R*)-ATPA. (*R*)-ATPO (0.2 mg, ee = 98.0%) (Møller et al., 1999) was refluxed in 48% aqueous hydrobromic acid (1.0 ml) for 90 min, evaporated, and re-evaporated from water. The residue was dissolved in water and analyzed using a 4.6 × 150-mm Chirobiotic T column connected to the same HPLC system which was used for the (*S*)-pipecolic acid ligand-exchange column. The column was eluted at 0.5 ml/min with 15 mM ammonium acetate/acetic acid buffer (pH 4.0): ethanol (20:80).

2.4. Receptor binding assays

The membrane preparations used in all receptor binding experiments were prepared according to Ransom and Stec (1988). In all of the binding assays, 8–10 mg of original tissue was used pr. aliquot, and Tris–HCl (pH 7.4) was used as buffer unless otherwise stated. On the day of the experiment, membranes were thawed and homogenized in 40 volumes of buffer and centrifuged at 48,000 × *g* for 15 min. The resulting pellet was homogenized in 40 volumes of buffer and centrifuged at 48,000 × *g* for 15 min. This last step was repeated three times.

Affinity for AMPA receptors was determined using the ligands [^{3}H]AMPA as described by Honoré and Nielsen (1985), and [^{3}H]CNQX as described by Honoré et al. (1989) with the following modifications. Using 5 nM [^{3}H]AMPA as radioligand, aliquots (250 μl), in triplicate, were incubated for 1 h at 0°C. After filtration through GF/B filters, using a 96-well Packard FilterMate cell-harvester, filters were washed three times with 250 μl ice-cold buffer. Non-specific binding was determined in the presence of 1 mM (*S*)-Glu. The amount of [^{3}H]AMPA bound to the membranes was determined using a Packard TOPCOUNT, microplate scintillation counter with a counting efficiency of 25%. [^{3}H]CNQX binding was carried out

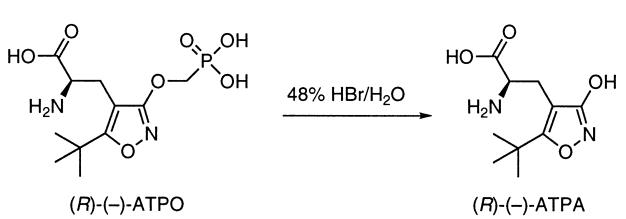

Fig. 3. Determination of the absolute stereochemistry of (*R*)-(−)-ATPA by the chemical conversion of (*R*)-(−)-ATPO, the stereochemistry of which has been established by an X-ray crystallographic analysis (Møller et al., 1999), into (*R*)-(−)-ATPA.

using 2 nM [^{3}H]CNQX in aliquots of 250 μl, in duplicates. After incubation for 45 min the assay was terminated by centrifugation at 18,500 × *g* for 3 min using a Sorvall FA-MICRO RMC-14 microcentrifuge. Pellets were rinsed three times with 1 ml ice-cold buffer, solubilized in 100 μl of 1% w/v sodium *n*-dodecylsulfate for 12 h, and added 1.1 ml scintillation liquid (Opti-fluor 0). The amount of [^{3}H]CNQX bound to the membranes were counted in a Packard TRI-CARB scintillation counter (model 2000 CA) with a counting efficiency of 65%.

[^{3}H]Kainic acid binding was performed as described by Braitman and Coyle (1987) with slight modifications. Aliquots (250 μl), in triplicate, were incubated for 1 h at 0°C. Instead of 1 nM [^{3}H]kainic acid, 5 nM [^{3}H]kainic acid was used, and the assay was terminated by filtration, using a 96-well Packard FilterMate cell-harvester, through GF/B filters, rather than by centrifugation. Filters were washed three times with 250 μl ice-cold buffer. Non-specific binding was determined in the presence of 1 mM (*S*)-Glu. The amount of [^{3}H]kainic acid bound to the membranes was determined using a Packard TOPCOUNT, microplate scintillation counter with a counting efficiency of 25%.

[^{3}H]CPP binding was studied following a procedure described by Murphy et al. (1987) with minor modifications. Aliquots (500 μl), in triplicate, were incubated for 30 min at 0°C, and termination of the assay was accomplished by filtration using a Brandell M-48R cell harvester through GF/B filters (presoaked in 0.1% polyethyleneimine), rather than by centrifugation. Filters were washed with 3 × 2 ml of buffer. The amount of [^{3}H]CPP bound to the membranes was determined using a Packard TRI-CARB scintillation counter (model 2000 CA) with a counting efficiency of 65%.

2.5. Rat cortical wedge preparation

A previously described rat cortical wedge preparation (Harrison and Simmonds, 1985) in a slightly modified version (Madsen et al., 1993) was used for the evaluation of the interaction of (*S*)- and (*R*)-ATPA with the native ionotropic (*S*)-Glu receptors. Agonists were applied for 90 s. In experiments examining antagonists, these were applied for 90 s prior to a 90-s co-application of agonist and antagonist.

2.6. Electrophysiology

Three to five ovarian lobes were surgically removed from anaesthetized *Xenopus laevis*. The removed ovaries were treated with collagenase type A (1 mg/ml, Boehringer) for 2–3 h at 20°C in buffer OR-2 (pH 7.6) consisting of 88 mM NaCl, 1.1 mM KCl, 2.4 mM $NaHCO_3$, 0.8 mM $MgCl_2$ and 15 mM HEPES-NaOH, and oocytes at stage V or VI were isolated. Oocytes were maintained in Barth's solution and injected the day after isolation with 5–30 ng cRNA and maintained in Barth's solution (buffer OR-2 supplemented with 0.3 mM $Ca(NO_3)_2$, 0.3 mM $CaCl_2$, 100 μg/ml gentamycin, 100 IU/ml penicillin, and 10 μg/ml streptomycin). Oocyte currents were recorded in Ringer solution (pH 7.5) consisting of 115 mM NaCl, 2.5 mM KCl, 1.8 mM $CaCl_2$, 0.1 mM $MgCl_2$, and 10 mM HEPES-NaOH, 3–14 days after injection using a two-electrode voltage clamp (Warner OC-725C). The pipettes had a resistance of 0.7–2 MΩ and were filled with 3 M KCl. Oocytes were clamped at −100–20 mV and for oocytes exhibiting currents larger than 500 nA the recordings were performed in low Ca^{2+} Ringer solution (pH 7.5) consisting of 115 mM NaCl, 2.5 mM, KCl, 0.1 mM $CaCl_2$, 1.8 mM $MgCl_2$, and 10 mM HEPES-NaOH, to avoid activation of the Ca^{2+} activated Cl^- current. The absence of Ca^{2+} activated Cl^- currents was assessed by a voltage ramp during activation of the largest response. The recordings of homomeric GluR5 and GluR6 receptors were performed after 10–15 min treatment with concanavalin A (1 mg/ml, Sigma type IV).

2.7. cRNA synthesis

Fragments only encoding the open reading frame of the different (*S*)-Glu receptors (GluR1-flop, GluR3-flop, GluR4-flop, GluR5-1a, GluR6, and KA2) were generated by polymerase chain reaction (PCR) and cloned into pGEMHE (Liman et al., 1992). The clones were verified by sequencing. cRNA transcripts were generated as runoff transcription on 20 μg/ml linerized plasmids by incubation in 40 mM Tris–HCl (pH 7.8), 8 mM $MgCl_2$, 2 mM spermidine, 50 mM NaCl, 3.5 mM DTT, 0.5 mM ATP, 0.5 mM UTP, 0.5 mM CTP, 0.1 mM GTP, 0.5 mM GpppG, and 0.5 U/μl T7 polymerase for 90 min in the presence of trace amounts of [^{32}P]UTP for quantification of the cRNA.

2.8. Data analysis

Binding data were analyzed by the nonlinear curve fitting program GRAFIT 3.0 (Leatherbarrow, 1992). Data were fitted to the equation: $B = 100 - (100 \times [\text{Inhibitor}]^n / (IC_{50}^n + [\text{Inhibitor}]^n))$, where B is the binding as a percentage of total specific binding and n the Hill coefficient. EC_{50} values were determined using the equation: % response $= (E_{max} \times [\text{Agonist}]^n)/(EC_{50}^n + [\text{Agonist}]^n)$, where E_{max} is the relative maximal response and n is the Hill coefficient. Biphasic dose–response curves were fitted to the equation: % response $= (E_{max(1)} \times [\text{Agonist}]^n)/(EC_{50(1)}^n + [\text{Agonist}]^n) + (100 - E_{max(1)} \times [\text{Agonist}]^n)/(EC_{50(2)}^n + [\text{Agonist}]^n)$. K_i values were estimated using the equation $\text{Log}(\text{DR}-1) = \alpha \text{Log}[\text{Antagonist}] + \text{p}K_i$; $\alpha = 1$, where DR is the dose ratio estimated by the following equation $\text{DR} = EC_{50}$ (Agonist)/EC_{50} (Agonist + Antagonist) under the assumption that the antagonism is competitive (Schild, 1947).

3. Results

3.1. Resolution and absolute stereochemistry of (R)-(−)-ATPA and (S)-(+)-ATPA

Racemic ATPA was resolved into (−)- and (+)-ATPA by a chiral HPLC separation using a Chirobiotic T column (Armstrong et al., 1995). Even though the preparative enantioseparation was performed without complete baseline separation between the two enantiomers (Fig. 2A), both enantiomers were obtained in high stereochemical purity after recrystallization (Fig. 2B). The enantiomeric purity of the (+)-enantiomer was determined using an (*S*)-pipecolic acid column and was found to be > 99.8% ee. The (−)-enantiomer had an ee = 99.8% when assayed on a Chirobiotic T column.

For the configurational assignment of (−)- and (+)-ATPA, the (*R*)-enantiomer of the *O*-phosphonomethyl analogue, (*R*)-ATPO was used (Fig. 3). The absolute configuration of (*R*)-ATPO has previously been established through an X-ray crystallographic analysis (Møller et al., 1999). Cleavage of the phosphonomethoxy moiety of (*R*)-ATPO with strong acid resulted in the formation of (*R*)-ATPA, and using chiral HPLC analyses, it was shown that (*R*)-ATPA formed from (*R*)-ATPO had the same UV-profile and co-eluted with the (−)-ATPA enantiomer, thus establishing the absolute configuration of (−)-ATPA. Under the chromatographic conditions used neither of the two ATPO enantiomers was retained ($k' < 0.5$) whereas (+)- and (−)-ATPA were well retained ($k' = 2.0$ and 3.3, respectively). Thus, (*R*)-(−)-ATPA is the late eluting of the ATPA enantiomers on the Chirobiotic T column and the first-eluting enantiomer on the (*S*)-pipecolic acid ligand-exchange column. These observed elution orders are in agreement with the general elution orders for racemic α-amino acids on these two types of chiral HPLC columns (Gübitz et al., 1981b; Berthod et al., 1996). CD-spectra of the two enantiomers were in agreement with what has previously been observed for enantiopure isoxazole containing α-amino acids, the (*R*)-enantiomer and (*S*)-enantiomer showing a negative and positive Cotton effect around 220 nm, respectively (Johansen et al., 1997; Falch et al., 1998).

3.2. Binding experiments

The affinities for AMPA receptors of (*R*)- and (*S*)-ATPA were tested using the radioligands [^{3}H]AMPA and [^{3}H]CNQX. (*R*)-ATPA did not show significant binding using [^{3}H]AMPA as the radioligand ($IC_{50} > 100$ μM), but had weak affinity for [^{3}H]CNQX binding sites ($IC_{50} = 50$ μM) (Table 1). (*R*)-ATPA was devoid of affinity when using either [^{3}H]kainic acid or the NMDA antagonist [^{3}H]CPP as radioligand. (*S*)-ATPA was found to have approximately twice the affinity of ATPA when using either [^{3}H]AMPA or [^{3}H]kainic acid as the radioligand, but was devoid of affinity for [^{3}H]CNQX or [^{3}H]CPP labelled binding sites.

3.3. Rat cortical wedge pharmacology

Using the rat cortical wedge preparation as an in vitro electrophysiological model, the two enantiomers of ATPA were tested for functional activities at native (*S*)-Glu receptors (Table 1 and Fig. 4). (*S*)-ATPA ($EC_{50} = 23$ μM) was found to be twice as potent as ATPA ($EC_{50} = 48$ μM (Ebert et al., 1992)), and responses elicited by 25 μM (*S*)-ATPA could be antagonized by 5 μM NBQX. (*R*)-ATPA did not show any depolarizing effects when tested up to 1 mM, but was found to have antagonistic effects. (*R*)-ATPA dose-dependently antagonized responses induced by AMPA with a K_i value = 253 μM. Responses produced by (*S*)-ATPA could also be antagonized by (*R*)-ATPA, but with a K_i value of 376 μM, which was significantly ($P < 0.05$, *t*-test) different from the K_i value obtained when antagonizing AMPA with (*R*)-ATPA. These results suggest that AMPA and (*S*)-ATPA activate dissimilar receptor populations in the cortical wedge preparation. (*R*)-ATPA did not antagonize responses elicited by NMDA. Depolarizations induced by low concentrations kainic acid in the cortical wedge preparation are visually different from depolarizations by NMDA or AMPA receptor agonists. The responses become broader probably reflecting slower kinetics. When increasing the kainic acid concentration (> 10 μM), responses do, however, not differ from responses elicited by AMPA or NMDA receptor agonists. Depolarizations obtained by co-applying different concentrations of kainic acid (0.2, 0.5, 1, 2, 5, 10, 20, 30, 50, 100 and 200 μM) with a fixed concentration of (*R*)-ATPA were used when calculating the K_i values for the lower and upper part of the dose–response curve (Fig. 4D). Datapoints were fitted to an equation assuming two independent receptor populations as described in Section 2.8. K_i values were found to be 1115 μM and 301 μM, representing antagonism of the lower and upper part of the biphasic dose–response curve of kainic acid, respectively.

Table 1
Membrane receptor binding and rat cortical wedge electrophysiology

	IC_{50} (μM)				EC_{50} (μM)
	[^{3}H]AMPA	[^{3}H]CNQX	[^{3}H]Kainic acid	[^{3}H]CPP	Electrophysiology
AMPA	0.04 ± 0.02	18 ± 5	> 100	> 100	3.5 ± 0.2
ATPA	3.9 ± 0.6	> 100[a]	31 ± 1	> 100	48[a]
(*S*)-ATPA	1.8 ± 0.2	> 100	23 ± 1	> 100	23 ± 3
(*R*)-ATPA	> 100	50 ± 7	> 100	> 100	> 1000[b]

Values are mean ± S.E.M. of at least three individual experiments.
[a] Ebert et al. (1992).
[b] Antagonism of AMPA, (*S*)-ATPA, kainic acid ([Kainic acid] < 10 μM), kainic acid ([Kainic acid] > 10 μM); K_i (μM) = 53 ± 6, 376 ± 41, 1115 ± 32, 301 ± 13, respectively.

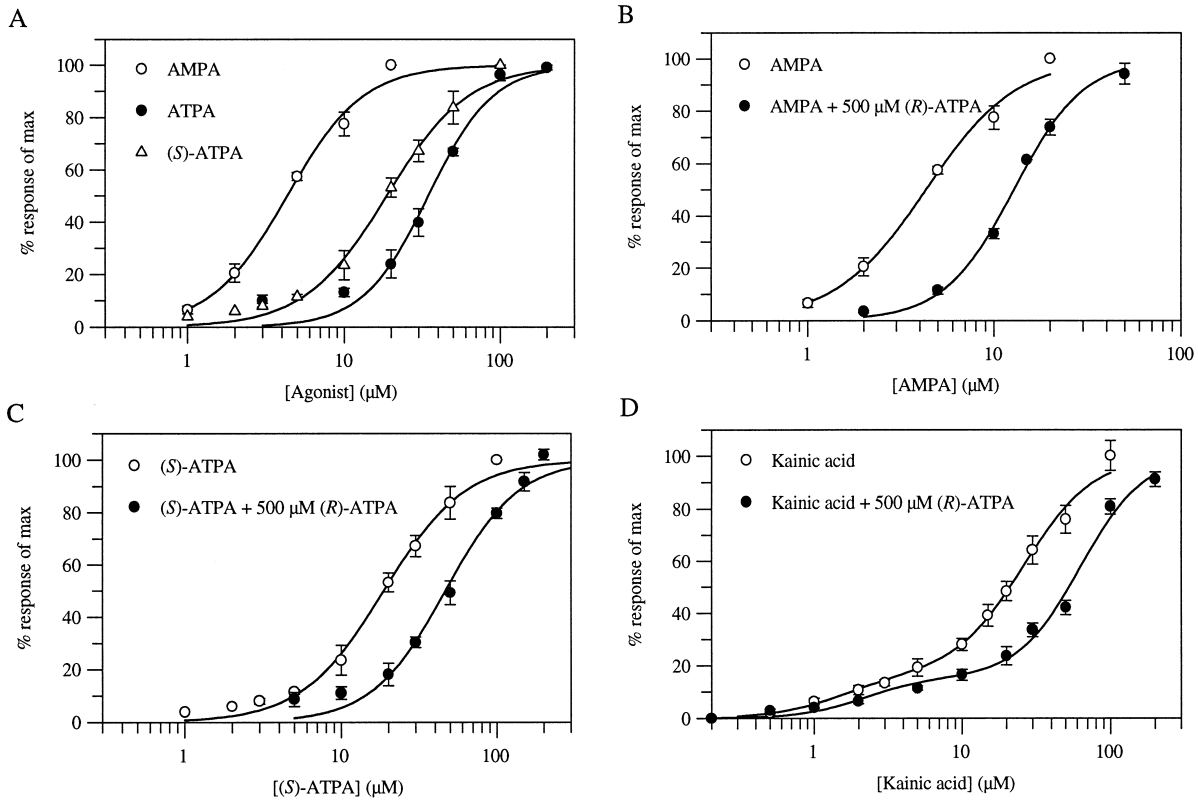

Fig. 4. Dose–response curves obtained in the cortical wedge preparation. (A) Curves showing the response elicited by increasing concentrations of AMPA (○), ATPA (●), and (*S*)-ATPA (Δ). (B) Antagonism of AMPA (○) with a fixed concentration of (*R*)-ATPA (500 μM) (●). (C) Antagonism of (*S*)-ATPA (○) with a fixed concentration of (*R*)-ATPA (500 μM) (●). (D) Antagonism of kainic acid (○) with a fixed concentration of (*R*)-ATPA (500 μM) (●).

3.4. Electrophysiological recordings

ATPA and (*S*)- and (*R*)-ATPA were tested on two electrode voltage clamped *Xenopus* oocytes expressing homomeric flop splice variants of the AMPA receptor subunits GluR1, GluR3, or GluR4 and oocytes expressing the homomeric kainic acid receptors GluR5-1a or GluR6 or the heteromeric combination GluR6 + KA2. The large size of the oocytes limits the rate of drug application. Consequently, the EC_{50} values are calculated from the steady-state currents induced by the compounds.

(*S*)-ATPA acts as an agonist at the AMPA receptors with EC_{50} values for GluR3 and GluR4 of approximately 8 μM, and a slightly higher EC_{50} value of 22 μM at GluR1

Table 2
Agonist and antagonist actions of ATPA and the enantiomers of ATPA at homomeric and heteromeric (*S*)-Glu receptor subtypes expressed in *Xenopus* oocytes

	ATPA			(*S*)-ATPA			(*R*)-ATPA	
	EC_{50} (μM)	n_H	Relative efficacy	EC_{50} (μM)	n_H	Relative efficacy	IC_{50} (μM)	K_i (μM)
GluR1	62 ± 6	0.61	0.20 ± 0.02	22 ± 5	1.6	0.3 ± 0.1	75 ± 10	33
GluR3	19 ± 4	0.97	0.064 ± 0.018	7.9 ± 1.3	0.84	0.054 ± 0.002	118 ± 16	75
GluR4	26 ± 3	0.77	0.18 ± 0.05	7.6 ± 2.0	0.67	0.33 ± 0.05	97 ± 6	52
GluR5	0.66 ± 0.06	1.1	0.9 ± 0.1	0.48 ± 0.06	1.0	0.96 ± 0.08	n.i.	
GluR6	n.r.			n.r.			n.i., n.r.	
GluR6 + KA2	155 ± 11	2	0.035 ± 0.001	61 ± 3	2.0	0.033 ± 0.002	n.i., n.r.	

Values are mean ± S.E.M. of at least three individual experiments.
The relative efficacy was measured as the maximal response induced by ATPA relative to 300 μM kainic acid for the AMPA receptors, 100 μM kainic acid at GluR5 receptors, and 50 μM AMPA at GluR6 + KA2 receptors. n.r.: No response at 600 μM. n.i.: No inhibition of kainic acid-induced current on GluR5 (10 μM) or GluR6 (1 μM) or 50 μM AMPA induced current on GluR6 + KA2.

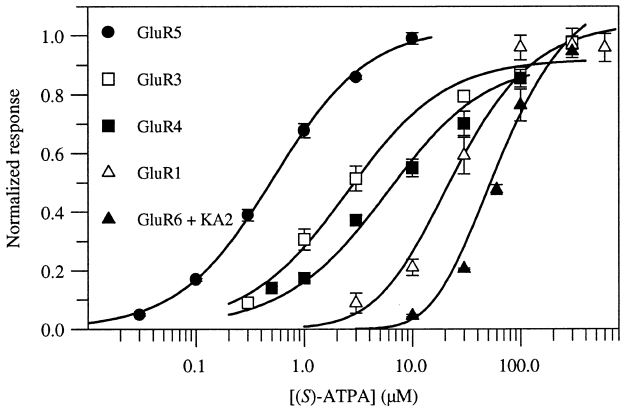

Fig. 5. Normalized dose–response curves of (*S*)-ATPA on recombinant AMPA-preferring (GluR1, GluR3, and GluR4) and kainic acid-preferring (GluR5 and GluR6+KA2) (*S*)-Glu receptors expressed in *Xenopus* oocytes.

(Table 2; Fig. 5). In accordance with this, racemic ATPA elicits responses approximately half the potency found for the (*S*)-enantiomer (Table 2). The maximal current evoked by (*S*)-ATPA is 30% at GluR1 and 33% at GluR4 receptors of the maximal kainic acid-induced current, while it is 5.4% at GluR3 (Table 2). Racemic ATPA showed maximal current amplitudes in the same ranges (Table 2). (*R*)-ATPA at 600 μM did not activate a current on the AMPA receptors (data not shown). However, (*R*)-ATPA antagonized kainic acid (30 μM) induced currents with K_i values between 33 and 75 μM (Fig. 6A; Table 2).

ATPA and (*S*)- and (*R*)-ATPA were studied on the GluR5-1a splice variant of the kainic acid-preferring GluR5 receptor (Bettler et al., 1990; Sommer et al., 1992). Although the desensitization was reduced by extensive treatment of the oocytes with concanavalin A prior to an agonist application, a significant desensitization was observed for (*S*)-ATPA at concentrations > 1 μM implied by a reduction in the current amplitude of the following application of 10 μM kainic acid. Consequently, the ATPA induced currents were normalized to subsequent application of 10 μM kainic acid. Alternating applications of 3 μM ATPA and 10 μM kainic acid revealed that this normalization adequately corrected for the induced desensitization. ATPA and (*S*)-ATPA were highly potent agonists on GluR5 with EC_{50} values of 0.66 ± 0.06 μM and 0.48 ± 0.06 μM, respectively. The maximal responses were not significantly different from the maximal kainic acid induced current (Table 2). (*R*)-ATPA at 300 μM did not antagonize the current induced by 10 μM kainic acid significantly (Fig. 6B). A weak agonist effect of (*R*)-ATPA at 600 μM was, however, observed (Fig. 6B). A likely explanation for this effect might be contamination of (*S*)-ATPA in the (*R*)-ATPA preparation, since 0.034 μM (*S*)-ATPA, equivalent to 0.006% of (*S*)-ATPA in the (*R*)-ATPA preparation, could evoke a similar current. Six hundred micromolars of ATPA or the enantiomers of ATPA did not activate any currents on the homomeric GluR6 receptors. Neither did similar concentrations antagonize the current induced by 1 μM kainic acid at GluR6 receptors.

The heteromeric GluR6 + KA2 combination was activated by ATPA and (*S*)-ATPA (Table 2) but (*R*)-ATPA (600 μM) did not exhibit any effects. Normalized to the

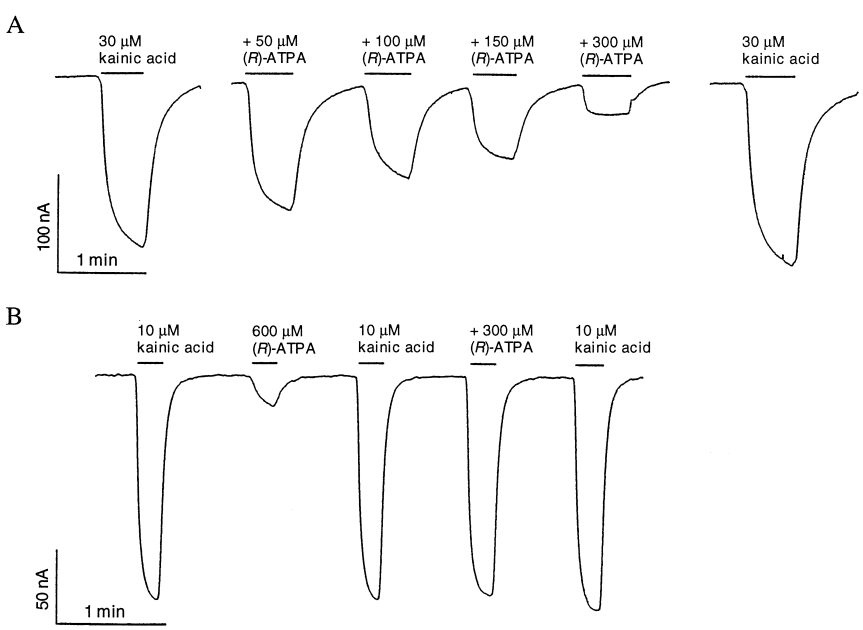

Fig. 6. Current traces of two electrode voltage clamped *Xenopus* oocytes. (A) Traces from oocytes expressing GluR3 after application of 30 μM kainic acid alone or in combination with different concentrations of (*R*)-ATPA. (B) Traces from oocytes expressing GluR5 and treated with concanavalin A to reduce desensitization. (*R*)-ATPA was applied alone or in combination with 10 μM kainic acid.

calculated maximal AMPA response ($EC_{50} = 111 \pm 5$ μM, $n_H = 1.8$, data not shown), the maximal response on the GluR6 + KA2 receptor combination of (*S*)-ATPA relative to 50 μM AMPA is 3.3 ± 0.2%.

4. Discussion

A prerequisite for studies of the physiological and patho-physiological roles of (*S*)-Glu receptors in the CNS at the molecular level is the availability of ligands with highly selective effects on subtypes of these receptors. Such compounds not only are indispensable tools for physiological and receptor mechanistic studies, but they also represent the initial steps in the rational design of therapeutic agents with effects on key receptor targets in CNS diseases (Krogsgaard-Larsen et al., 1996).

ATPA, which contains a bulky and lipophilic *tert*-butyl group (Fig. 1), was originally designed as a model structure for mapping of the topography of the agonist recognition sites of the AMPA receptors and as a pharmacological tool capable of penetrating the blood–brain barrier (Krogsgaard-Larsen et al., 1982; Lauridsen et al., 1985). ATPA actually has been shown to be active after systemic administration in animals (Turski et al., 1992; Arnt et al., 1995). Whereas the *tert*-butyl group appears to represent the maximal size of a C-5 AMPA substituent tolerated by AMPA receptor agonist sites (Sløk et al., 1997), this group appears to be easily, and perhaps optimally, accommodated at the agonist recognition site of the kainic acid-preferring (*S*)-Glu receptor, GluR5 (Wahl et al., 1998), where ATPA has been shown to be a very potent agonist (Clarke et al., 1997). ATPA has been described as the most selective GluR5 agonist so far available (Chittajallu et al., 1999).

In light of these recent findings, we decided to study the relationship between the absolute stereochemistry of the enantiomers of ATPA and their brain tissue pharmacology, using the rat cortical wedge model, and molecular pharmacology, using cloned subtypes of AMPA- and kainic acid-preferring (*S*)-Glu receptors. In the former test system, (*S*)-ATPA showed agonist effects, whereas (*R*)-ATPA was shown to antagonize the depolarizing effects of (*S*)-ATPA as well as AMPA. Using cloned subtypes of (*S*)-Glu receptors, the agonist effects of (*S*)-ATPA were shown to be mediated by AMPA-preferring receptors (GluR1, GluR3, and GluR4) and, in particular, by the kainic acid preferring receptor, GluR5, whereas the antagonistic effects of (*R*)-ATPA were mediated exclusively by AMPA receptor subtypes.

The K_i value obtained when antagonizing (*S*)-ATPA with (*R*)-ATPA was found to be 376 μM in the rat cortical wedge preparation. This value is significantly different ($P < 0.05$, *t*-test) from that obtained when antagonizing AMPA with (*R*)-ATPA ($K_i = 253$ μM), thus indicating that AMPA and (*S*)-ATPA mediate responses through different receptor populations in the native receptors present in the rat cortical wedge preparation. As depicted in Fig. 4D, the dose–response curve obtained from kainic acid applications is biphasic, although curvefits assuming two independent receptor populations are not fitted significantly better to the data than curvefits assuming one receptor population ($P > 0.05$). Antagonizing the responses by kainic acid with (*R*)-ATPA, two different K_i values were obtained. One K_i value (1115 μM) representing the antagonism of the lower part of the dose–response curve of kainic acid ([kainic acid] < 10 μM), and another K_i value (301 μM) representing the antagonism of the upper part of the dose–response curve ([kainic acid] > 10 μM). In the presence of the antagonist (*R*)-ATPA curvefits assuming two independent receptor populations fit the data significantly better than curvefits only assuming one receptor population ($P < 0.05$). We believe that the lower part of the kainic acid dose–response curve reflects interaction with kainic acid-preferring receptors, whereas the upper part reflects interaction with AMPA-preferring receptors. Thus, (*R*)-ATPA seems to interact selectively with AMPA-preferring receptors.

The electrophysiological characterizations of the compounds on recombinant receptors revealed that (*S*)-ATPA is a potent agonist on the (*S*)-Glu receptors with roughly 20-fold higher potency at homomeric GluR5 than at the homomeric flop splice variants of the AMPA receptors (GluR1, GluR3, and GluR4). We observed an EC_{50} of 0.48 μM for (*S*)-ATPA and 0.66 μM for ATPA on GluR5 receptors treated with concanavalin A. The latter is comparable with EC_{50} values of 2.1 μM and 0.62 μM observed in human embryonic kidney (HEK) 293 cells transfected with human GluR5 and rat DRG neurons, respectively (Clarke et al., 1997). However, we find that the EC_{50} values of ATPA on AMPA receptors are between 19 μM and 62 μM, which indicate 6–25-fold higher potency of ATPA than observed in HEK 293 cells transfected with the human AMPA receptor encoding clones (Clarke et al., 1997). Our measurements are based on the ATPA induced steady-state current which might be the most relevant parameter for investigations in animal or other conditions with slow application. Indeed, we find a very good agreement between the cortical wedge model EC_{50} value of 48 μM and the EC_{50} values from the oocyte recordings.

In conclusion, we have demonstrated that the agonist effect of the AMPA analogue, ATPA, at inotropic (*S*)-Glu receptors exclusively resides in (*S*)-ATPA, which is markedly more potent at the kainic acid-preferring GluR5 receptor than at the AMPA receptor subtypes (GluR1, GluR3, and GluR4), but inactive at GluR6, which like GluR5 is selectively activated by kainic acid. It is concluded that the bulky *tert*-butyl group of (*S*)-ATPA is much better accommodated by GluR5 than by GluR1, GluR3, GluR4 or GluR6. Nevertheless, (*R*)-ATPA is rec-

ognized as an antagonist by the AMPA receptor subtypes, but not detectably by GluR5 or GluR6. These stereostructure-activity relationships may be useful for the design of new selective/specific agonists or antagonists for subtypes of AMPA- and kainic acid-preferring (*S*)-Glu receptors.

Acknowledgements

This work was supported by grants from the Lundbeck Foundation, the Carlsberg Foundation, and from the Danish Medical Research Council. The secretarial assistance of Mrs. Anne Nordly is gratefully acknowledged.

References

Armstrong, D.W., Liu, Y., Ekborgott, K.H., 1995. A covalently bonded teicoplanin chiral stationary phase for HPLC enantioseparations. Chirality 7, 474–497.

Arnt, J., Sánchez, C., Lenz, S.M., Madsen, U., Krogsgaard-Larsen, P., 1995. Differentiation of in vivo effects of AMPA and NMDA receptor ligands using drug discrimination methods and convulsant/anticonvulsant activity. Eur. J. Pharmacol. 285, 289–297.

Berthod, A., Liu, Y., Bagwill, C., Armstrong, D.W., 1996. Facile liquid chromatographic enantioresolution of native amino acids and peptides using teicoplanin chiral stationary phase. J. Chromatogr. 731, 123–137.

Bettler, B., Boulter, J., Hermans-Borgmeyer, I., O'Shea-Greenfield, A., Deneris, E.S., Borgmeyer, U., Hollmann, M., Heinemann, S., 1990. Cloning of a novel glutamate receptor subunit, GluR5: expression in the nervous system during development. Neuron 5, 583–595.

Braitman, D.J., Coyle, J.T., 1987. Inhibition of [^{3}H]kainic acid receptor binding by divalent cations correlates with ion affinity for the calcium channel. Neuropharmacology 26, 1247–1251.

Chittajallu, R., Braithwaite, S.P., Clarke, V.R.J., Henley, J.M., 1999. Kainate receptors: subunits, synaptic localization and function. Trends Pharmacol. Sci. 20, 26–35.

Clarke, V.R.J., Ballyk, B.A., Hoo, K.H., Mandelzys, A., Pellizzari, A., Bath, C.P., Thomas, J., Sharpe, E.F., Davies, C.H., Ornstein, P.L., Schoepp, D.D., Kamboj, R.K., Collingridge, G.L., Lodge, D., Bleakman, D., 1997. A hippocampal GluR5 kainate receptor regulating inhibitory synaptic transmission. Nature 389, 599–603.

Collingridge, G., Watkins, J.C., 1994. The NMDA Receptor. Oxford Univ. Press, Oxford.

Conn, P.J., Pin, J.-P., 1997. Pharmacology and functions of metabotropic glutamate receptors. Ann. Rev. Pharmacol. Toxicol. 37, 205–237.

Curry, K., Pajouhesh, H., 1998. Pharmacological profile of the isomers of the GluR-specific agonist ATPA. Can. J. Physiol. Pharmacol. 76, 690–692.

Danysz, W., Parsons, C.G., Bresink, I., Quack, G., 1995. Glutamate in CNS disorders. Drug News & Perspect. 8, 261–277.

Ebert, B., Madsen, U., Lund, T.M., Holm, T., Krogsgaard-Larsen, P., 1992. Molecular pharmacology of cortical and spinal AMPA receptors. Mol. Neuropharmacol. 2, 47–49.

Falch, E., Brehm, L., Mikkelsen, I., Johansen, T.N., Skjærbæk, N., Nielsen, B., Stensbøl, T.B., Ebert, B., Krogsgaard-Larsen, P., 1998. Heteroaryl analogues of AMPA: 2. Synthesis, absolute stereochemistry, photochemistry and structure-activity relationships. J. Med. Chem. 41, 2513–2523.

Gübitz, G., Jellenz, W., Santi, W., 1981a. Resolution of the optical isomers of underivatisized amino acids on chemically bound chiral phases by ligand exchange chromatography. J. Liq. Chromatogr. 4, 701–712.

Gübitz, G., Jellenz, W., Santi, W., 1981b. Resolution of the optical isomers of amino acids by ligand-exchange chromatography using chemically bonded chiral phases. J. Chromatogr. 203, 377–384.

Harrison, N.L., Simmonds, M.A., 1985. Quantitative studies on some antagonists of *N*-methyl-D-aspartate in slices of rat cerebral cortex. Br. J. Pharmacol. 84, 381–391.

Hollmann, M., Heinemann, S., 1994. Cloned glutamate receptors. Annu. Rev. Neurosci. 17, 31–108.

Honoré, T., Nielsen, M., 1985. Complex structure of quisqualate-sensitive glutamate receptors in rat cortex. Neurosci. Lett. 54, 27–32.

Honoré, T., Drejer, J., Nielsen, E.Ø., Nielsen, M., 1989. Non-NMDA glutamate receptor antagonist ^{3}H-CNQX binds with equal affinity to two agonist states of quisqualate receptors. Biochem. Pharmacol. 38, 3207–3212.

Johansen, T.N., Ebert, B., Falch, E., Krogsgaard-Larsen, P., 1997. AMPA receptor agonists: resolution, configurational assignment, and pharmacology of (+)-(S)- and (−)-(R)-2-amino-3-[3-hydroxy-5-(2-pyridyl)-isoxazol-4-yl]-propionic acid (2-Py-AMPA). Chirality 9, 274–280.

Knöpfel, T., Kuhn, R., Allgeier, H., 1995. Metabotropic glutamate receptors: novel targets for drug development. J. Med. Chem. 38, 1417–1426.

Krogsgaard-Larsen, P., Hansen, J.J., Lauridsen, J., Peet, M.J., Leah, J.D., Curtis, D.R., 1982. Glutamic acid agonists, stereochemical and conformational studies of DL-α-amino-3- hydroxy-5-methyl-4-isoxazolepropionic acid (AMPA) and related compounds. Neurosci. Lett. 31, 313–317.

Krogsgaard-Larsen, P., Ebert, B., Lund, T.M., Bräuner-Osborne, H., Sløk, F.A., Johansen, T.N., Brehm, L., Madsen, U., 1996. Design of excitatory amino acid receptor agonists, partial agonists and antagonists: ibotenic acid as a key lead structure. Eur. J. Med. Chem. 31, 515–537.

Lauridsen, J., Honoré, T., Krogsgaard-Larsen, P., 1985. Ibotenic acid analogues. Synthesis, molecular flexibility, and in vitro activity of agonists and antagonists at central glutamic acid receptors. J. Med. Chem. 28, 668–672.

Leatherbarrow, R.J., 1992. GraFit version 3.0. Erithacus Software, Staines, U.K.

Liman, E.R., Tytgat, J., Hess, P., 1992. Subunit stoichiometry of mammalian K^+ channel determined by construction of multimeric cDNAs. Neuron 9, 671–861.

Madsen, U., Frølund, B., Lund, T.M., Ebert, B., Krogsgaard-Larsen, P., 1993. Design, synthesis and pharmacology of model compounds for indirect elucidation of the topography of AMPA receptor sites. Eur. J. Med. Chem. 28, 791–800.

Monaghan, D.T., Wenthold, R.J. 1997. The Inotropic Glutamate Receptors. Humana Press, Totowa, NJ.

Murphy, D.E., Schneider, J., Boehm, C., Lehmann, J., Williams, M., 1987. Binding of [^{3}H]3-(2-carboxypiperazin-4yl)propyl-1-phosphonic acid to rat brain membranes: a selective, high-affinity ligand for *N*-methyl-D-aspartate receptors. J. Pharmacol. Exp. Ther. 240, 778–784.

Møller, E.H., Egebjerg, J., Brehm, L., Stensbøl, T.B., Johansen, T.N., Madsen, U., Krogsgaard-Larsen, P., 1999. Resolution, absolute stereochemistry, and enantiopharmacology of the GluR1-4 and GluR5 antagonist 2-amino-3-(5-tert-butyl-3-(phosphonomethoxy)-4-isoxazolyl)propionic acid. Chirality 11, in press.

Ransom, R.W., Stec, N.L., 1988. Cooperative modulation of [^{3}H]MK-801 binding to the *N*-methyl-D-aspartate receptor ion channel complex by L-glutamate, glycine and polyamines. J. Neurochem. 51, 830–836.

Schild, H.O., 1947. pA, A new scale for the measurement of drug antagonism. Br. J. Pharmacol. 2, 189–206.

Sløk, F.A., Ebert, B., Lang, Y., Krogsgaard-Larsen, P., Lenz, S.M., Madsen, U., 1997. Excitatory amino-acid receptor agonists. Synthesis and pharmacology of analogues of 2-amino-3-(3-hydroxy-5-methyl-isoxazol-4-yl)propionic acid. Eur. J. Med. Chem. 32, 329–338.

Sommer, B., Burnashev, N., Verdoorn, T.A., Kainanen, K., Sakmann, B.,

Seeburg, P.H., 1992. A glutamate receptor channel with high affinity for domoate and kainate. EMBO J. 11, 1651–1656.

Turski, L., Jacobsen, P., Honoré, T., Stephens, D.N., 1992. Relief of experimental spasticity and anxiolytic/anticonvulsant actions of the α-amino-3-hydroxy-5-methyl-4-isoxazole-propionate antagonist 2,3-dihydroxy-6-nitro-7-sulfamoylbenzo(F)quinoxaline. J. Pharmacol. Exp. Ther. 260, 742–747.

Wahl, P., Frandsen, A., Madsen, U., Schousboe, A., Krogsgaard-Larsen, P., 1998. Pharmacology and toxicology of ATOA, an AMPA receptor antagonist and a partial agonist at GluR5 receptors. Neuropharmacology 37, 1205–1210.

Wheal, H.V., Thomson, A.M., 1995. Excitatory Amino Acids and Synaptic transmission. Academic Press, London.